Nonequilibrium Mass Transport in the 1D Fermi-Hubbard Model

S. Scherg,[1,2] T. Kohlert,[1,2] J. Herbrych,[3,4] J. Stolpp,[1,5,6] P. Bordia,[1,2] U. Schneider,[1,2,7]
F. Heidrich-Meisner,[5] I. Bloch,[1,2] and M. Aidelsburger[1,2,*]

[1]*Fakultät für Physik, Ludwig-Maximilians-Universität München, Munich, Germany*
[2]*Max-Planck-Institut für Quantenoptik, 85748 Garching, Germany*
[3]*Department of Physics and Astronomy, University of Tennessee, Knoxville, Tennessee 37996, USA*
[4]*Materials Science and Technology Division Oak Ridge National Laboratory, Oak Ridge, Tennessee 37831, USA*
[5]*Institute for Theoretical Physics, Georg-August-Universität Göttingen, 37077 Göttingen, Germany*
[6]*Arnold Sommerfeld Center for Theoretical Physics, Ludwig-Maximilians-Universität München, 80333 Munich, Germany*
[7]*Cavendish Laboratory, University of Cambridge, Cambridge CB3 0HE, United Kingdom*

(Received 20 June 2018; revised manuscript received 21 August 2018; published 25 September 2018)

We experimentally and numerically investigate the sudden expansion of fermions in a homogeneous one-dimensional optical lattice. For initial states with an appreciable amount of doublons, we observe a dynamical phase separation between rapidly expanding singlons and slow doublons remaining in the trap center, realizing the key aspect of fermionic quantum distillation in the strongly interacting limit. For initial states without doublons, we find a reduced interaction dependence of the asymptotic expansion speed compared to bosons, which is explained by the interaction energy produced in the quench.

DOI: 10.1103/PhysRevLett.121.130402

Many-body physics in one dimension (1D) differs in numerous essential aspects from its higher-dimensional counterparts. Several familiar concepts, such as Fermi-liquid theory [1,2], are not applicable in 1D. Moreover, many 1D models are integrable, meaning that there exist exact solutions. Examples include the Lieb-Liniger model [3], the Heisenberg chain [4], or the 1D Fermi-Hubbard model (FHM) [5]. These models exhibit extensive sets of conserved quantities that prevent thermalization [6–11] and can, in lattice systems, lead to anomalous transport properties [12–15]. Cold-atom experiments offer the possibility to study transport properties of strongly correlated quantum gases in a clean environment. Their excellent controllability enabled far-from-equilibrium experiments [16–20] as well as close-to-equilibrium measurements in the linear-response regime [21–24] both in extended lattices and mesoscopic systems [25–27].

Here, we investigate mass transport in the 1D FHM in far-from-equilibrium expansion experiments [18–20], where an initially trapped gas is suddenly released into a homogeneous potential landscape as illustrated in Fig. 1. There are two distinct regimes of interest in sudden-expansion studies: the asymptotic one, where the expanding gas has become dilute and effectively noninteracting [28–36] and the transient regime, where the dynamical quasicondensation of hardcore bosons [37–41] and quantum distillation [20,42–44] have been found.

Quantum distillation occurs for large interactions. It relies on the dynamical demixing of fast singlons (one atom per site) and slow doublons (two atoms per site)

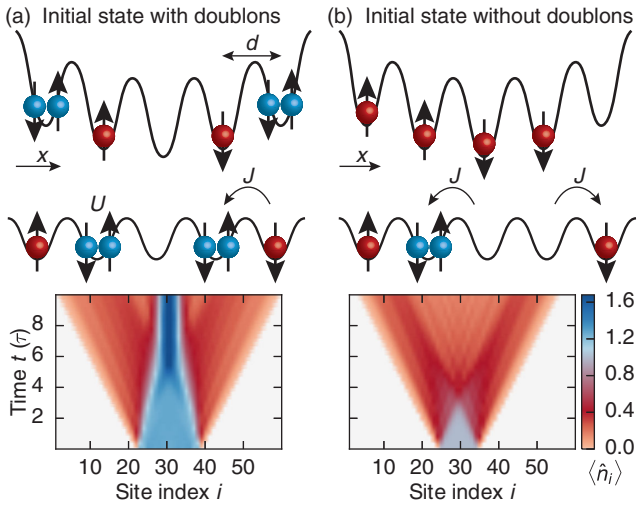

FIG. 1. Schematics of the expansion experiment. Top: Initial state of the harmonically trapped two-component Fermi gas with (a) singlons (red) and doublons (blue) and (b) only singlons in an optical lattice. After quenching to lower lattice depths and removing the harmonic trap, fermions expand in a homogeneous 1D lattice; $J = h \cdot 0.54(3)$ kHz denotes the tunnel coupling, U refers to the on-site interaction strength and d is the lattice constant. The expansion dynamics is dominated by first-order processes: (a) the resonant exchange of singlon and doublon positions leads to quantum distillation, (b) the dynamical formation of doublons results in reduced asymptotic expansion velocities. Bottom: Time-dependent density-matrix renormalization group (tDMRG) simulations of the atomic density $\langle \hat{n}_i \rangle$ for $U = 20J$ as a function of time t in units of the tunneling time $\tau = \hbar/J$.

during the expansion: while isolated doublons only move with a small effective second-order tunneling matrix element $J_{\mathrm{eff}} = 2J^2/U \ll J$ for $U \gg J$ [45,46], neighboring singlons and doublons can exchange their positions via fast, resonant first-order tunneling processes. Thus, after opening the trap, singlons escape from regions of the cloud initially occupied by singlons and doublons, leading to a spatial separation of the two components. Without an increase of the doublon density in the central region, this regime is termed weak quantum distillation [44]. Ideal initial-state conditions can lead to a strong version of quantum distillation, where the spatial separation of singlons and doublons yields a contraction of the doublon cloud radius [Fig. 1(a)]. In the extreme limit this distillation could be used to purify a finite-temperature band insulator [42], thereby dynamically generating low-entropy regions. This would represent a major advancement in the ongoing quest of realizing fermionic many-body physics at the lowest entropy scales [47–51]. So far, experimental evidence for weak quantum distillation has only been found for bosons [20] at intermediate interaction strengths, where doublons can decay into singlons on time scales relevant to quantum distillation.

In this work, we investigate the nonequilibrium mass transport in the 1D FHM starting from initial product states in deep optical lattices [18,19], while close-to-thermal initial states were used in Ref. [20]. The expansion dynamics is initiated by two simultaneous quenches: a sudden increase of the tunnel coupling, resulting in a quench from almost infinite to finite U/J, and a sudden removal of the harmonic trap (Fig. 1). We prepare initial product states with or without doublons (Fig. 1) and quantitatively investigate the time evolution of singlon and doublon densities individually. For initial states with doublons, we find a distinct dynamical phase separation between singlons and doublons, which is the fundamental mechanism of fermionic quantum distillation [Fig. 1(a)]. For initial states without doublons [Fig. 1(b)], we study interaction effects in the asymptotic expansion velocities [35]. We observe that the cloud expands rapidly at all interaction strengths with slightly smaller velocities at intermediate values, in agreement with our numerical simulations. This can be interpreted in terms of the interaction energy produced in the quench of U/J, which leads to the dynamical formation of doublons [19,33,52].

Experiment.—We prepare a degenerate Fermi gas of $30(1) \times 10^3$ ^{40}K atoms in a crossed dipole trap at the initial temperature $T/T_F = 0.15(1)$, where T_F is the Fermi temperature. The gas consists of an equal mixture of two spin components corresponding to the states $|\uparrow\rangle = |m_F = -7/2\rangle$ and $|\downarrow\rangle = |m_F = -9/2\rangle$ in the $F = 9/2$ hyperfine ground-state manifold. Our sequence begins with loading the atoms into a blue-detuned three-dimensional optical lattice with wavelength $\lambda_x = 532$ nm and lattice constant $d = \lambda_x/2$ along the x direction and $\lambda_\perp = 738$ nm in the transverse directions. While the main lattice along x is initially loaded to 20 E_{rx}, the transverse lattices are simultaneously ramped to a depth of $33E_{r\perp}$, where they remain during the whole sequence to realize individual 1D systems. Here, $E_{rj} = \hbar^2 k_j^2/(2m)$ are the respective recoil energies with $j \in \{x, \perp\}$, $k_j = 2\pi/\lambda_j$ denotes the corresponding wave vector, and m is the mass of ^{40}K. Holding the atoms in the deep initial lattice for 20 ms dephases remaining correlations between neighboring sites, such that the resulting state can be approximated as a product state $|\psi_0\rangle = \prod_{i\in\mathrm{trap}} (\hat{c}_{i\uparrow}^\dagger)^{n_{i\uparrow}} (\hat{c}_{i\downarrow}^\dagger)^{n_{i\downarrow}} |0\rangle$, where $\hat{c}_{i\sigma}^\dagger$ is the fermionic creation operator, $n_{i\sigma} \in \{0, 1\}$, $\sigma \in \{\uparrow, \downarrow\}$, and i is the lattice-site index. The spin orientations are expected to be distributed randomly among the sites and the average number of atoms per lattice site in the center of the cloud $\langle \hat{n}_i \rangle = \sum_\sigma \langle \hat{n}_{i\sigma} \rangle$ is estimated to be $\langle \hat{n}_i \rangle \lesssim 0.9$ [53], $\hat{n}_{i\sigma} = \hat{c}_{i\sigma}^\dagger \hat{c}_{i\sigma}$ is the density operator. The fraction of atoms on doubly occupied sites $n_d = N_d/(N_s + N_d)$ in the initial state can be tuned via the interaction strength during the loading process employing a Feshbach resonance at 202.1 G [53]. Here, $N_s(N_d)$ denotes the number of particles on singly (doubly) occupied sites. The dynamics starts with suddenly quenching the main lattice to 8 E_{rx}. Simultaneously, the strength of the dipole trap is adjusted to compensate the anticonfining harmonic potential introduced by the lattice [53]. Our system is then described by the homogeneous 1D FHM

$$\hat{H} = -J \sum_{i,\sigma=\uparrow,\downarrow} (\hat{c}_{i\sigma}^\dagger \hat{c}_{i+1\sigma} + \mathrm{H.c.}) + U \sum_i \hat{n}_{i\uparrow} \hat{n}_{i\downarrow}. \quad (1)$$

After a variable expansion time t the on-site population is frozen by suddenly increasing the lattice depth to 20 E_{rx}. Subsequently, the cloud is imaged *in situ* using high-field imaging either with or without removing doublons [53]. By combining these images, the dynamics of singlons and doublons can be resolved individually.

Quantum distillation.—We characterize the dynamics by monitoring the singlon and doublon clouds as a function of the expansion time for an initial state with $n_d = 0.40(2)$ [Figs. 2(a), 2(b)]. Isolated doublons are expected to become stable objects for interaction strengths that are large compared to the bandwidth $U \gg W$, $W = 4J$ [63], since in this case the interaction energy released in the doublon decay cannot be transferred into kinetic energy of singlons in low-order processes [45,63]. This is in agreement with our observations [insets in Figs. 2(a), 2(b)], where for $U = 5J$ we witness a fast doublon decay of about 25% in the early stages of the expansion $t \lesssim 5\tau$, which is accompanied by a compatible increase of the singlon number. In contrast, both numbers remain approximately constant for $U = 20J$. Except for a small residual decay, which is attributed to light-assisted losses of doublons [64], this enables us to probe the dynamical phase separation of singlons and doublons at approximately constant doublon numbers.

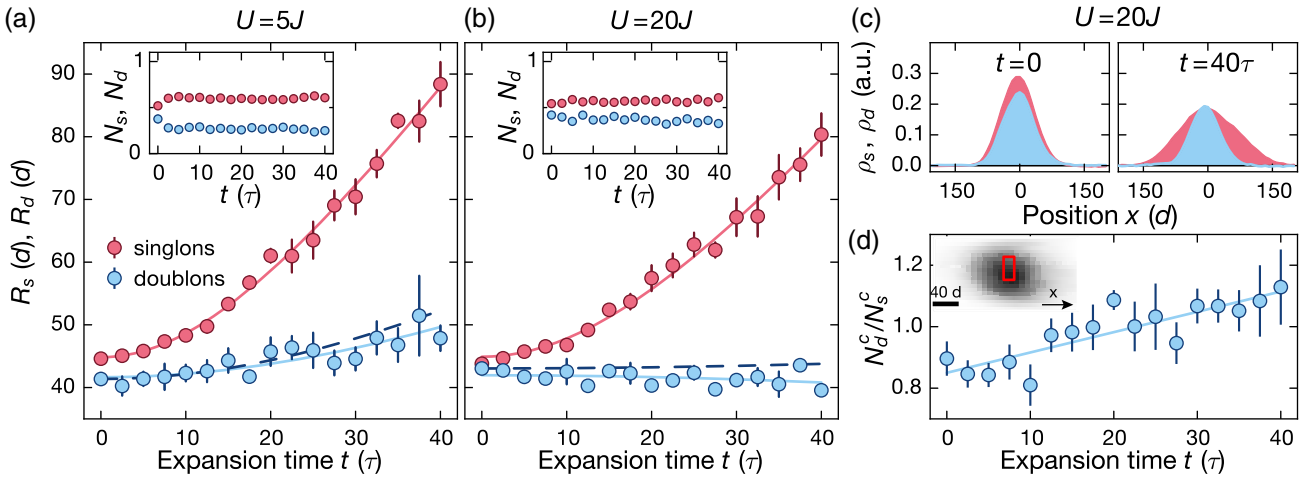

FIG. 2. Dynamical phase separation of singlons and doublons. Half-width-at-half-maximum (HWHM) size $R_{s,d}$ of singlon (s, red) and doublon (d, blue) clouds as a function of time for (a) $U = 5J$ and (b) $U = 20J$. The dashed lines illustrate the hypothetical expansion of a noninteracting doublon cloud with effective tunneling J_{eff} [53]. Insets: Number of atoms on singly and doubly occupied sites, N_s and N_d, as a function of time. (c) Experimental snapshots of the integrated line densities for singlon and doublon clouds, $\rho_s(x)$ and $\rho_d(x)$, at $t = 0$ (left) and $t = 40\tau$ (right). (d) Ratio N_d^c/N_s^c of atom numbers on doubly and singly occupied sites in the central region of the cloud (red rectangle in the inset) as a function of time for $U = 20J$. Every data point is averaged over four measurements and error bars represent the standard error of the mean. Solid lines are guides to the eye.

We study the phase separation by extracting the cloud sizes $R_{s,d}(t)$ at half-width-at-half maximum (HWHM). We observe a rapidly expanding singlon cloud, which has approximately doubled in size at $t = 40\tau$. In contrast, the doublon cloud size grows much slower and we even observe a weak shrinking of the cloud for $U = 20J$. For comparison, we show the expected expansion of a fictitious cloud of noninteracting doublons expanding according to J_{eff} [46]. The difference highlights the nontrivial nature of this transient dynamics. The dynamical phase separation is even more evident in the comparison of the integrated line densities of singlons and doublons at $t = 0$ and $t = 40\tau$ for our strongest interactions [Fig. 2(c)]. Clearly, the singlons expand significantly, while the doublons essentially remain in the center of the cloud. As a consequence, the ratio of atom numbers on doubly and singly occupied sites N_d^c/N_s^c in the center of the cloud increases by about 40% [Fig. 2(d)]. While this signal could in principle be caused by 1D systems with a low doublon fraction, a quantitative analysis based on our measured initial density distributions shows that their contribution to the signal is negligible [53]. Hence, our data establish clear evidence for fermionic quantum distillation in the weak regime in a nonequilibrium mass-transport experiment.

tDMRG results for transient dynamics.—Quantum distillation in the strong regime can further lead to a shrinking of the doublon cloud. The precise amount depends on the number of singlons initially confined in the doublon cloud, the initial density, and the cloud size [42,44,53]. Here, we focus on the role of the initial density, which has the largest influence. Figure 3 shows tDMRG simulations of the relative change of the doublon cloud size $\Delta R_d(t) = R_d(t)/R_d(0) - 1$ as a function of time for different average initial densities $n = (N_s + N_d)/L_{\mathrm{init}}$ in an ideal box trap of length L_{init} for constant $n_d = 0.4$ [53]. Negative values of ΔR_d indicate a shrinking of the doublon cloud, while $\Delta R_d > 0$ corresponds to an expanding doublon cloud. For the initial state with the largest density

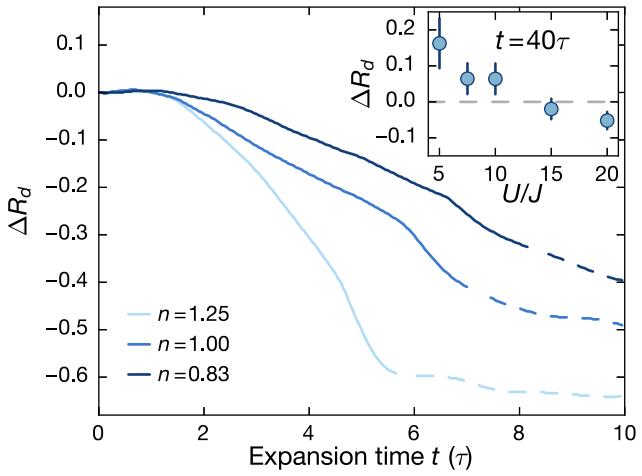

FIG. 3. tDMRG results for the relative doublon cloud size. Main panel: Relative doublon cloud size $\Delta R_d(t)$ for three different initial uniform densities n at $U/J = 20$. The initial state consists of 12 singlons, 4 doublons, and $\{0, 4, 8\}$ holons, respectively [53]. The solid lines end at time t_{max}, when the width of the singlon cloud increased to $\Delta R_s = 0.8$. This value corresponds to the experimental one at $t = 40\tau$. Inset: Experimental data for ΔR_d as a function of the interaction strength at $t = 40\tau$, which was evaluated using linear fits to the time traces $R_d(t)$ as shown in Figs. 2(a), 2(b) [53].

$n = 1.25$, we observe a large decrease of $\Delta R_d(t)$. This effect is substantially reduced for smaller densities (Fig. 3) due to the presence of holons (empty sites), which remain trapped between doublons on the time scales of the quantum distillation process [44]. Additionally, the dynamics becomes slower, both due to holons and due to the larger cloud sizes used for simulations with smaller average densities [44]. Despite these quantitative differences, however, we find that the fundamental aspect of quantum distillation, i.e., the dynamical phase separation of singlons and doublons, is generally robust.

For comparison, we show the experimentally measured relative changes ΔR_d as a function of interaction strength [inset in Fig. 3]. For all interactions the time traces of the doublon HWHM are fitted with a linear function to calculate ΔR_d at the maximum expansion time $t = 40\tau$ [53]. We observe that $\Delta R_d(40\tau)$ approaches zero with increasing interaction strength and becomes slightly negative at $U/J = 20$. In order to facilitate a comparison between experiment and numerics, where much smaller particle numbers are used, we define a time $t_{\max}$ for the simulation at which the relative singlon cloud size ΔR_s has reached the same value as in the experiment (Fig. 3). Our numerical results indicate that the contraction is not completed at this time. In the experiment this time is limited by the degree of flatness of the homogeneous potential. The remaining difference between the numerical and experimental results is most likely due to other initial-state properties, such as inhomogeneous density distributions and the averaging over several 1D systems with different initial-state properties [53].

Asymptotic dynamics and interaction effects.—Here, we focus on the dynamics of the whole cloud for initial states with a negligible doublon fraction ($n_d < 0.05$). We extract the second moment $r^2 = \sum_i \langle \hat{n}_i \rangle (i_0 - i)^2 d^2/(N_s + N_d)$ of the time-dependent density distribution (see Ref. [53] for details on the analysis), which is routinely computed in numerical simulations [32,33,35]; here i_0 is the center of mass of the initially trapped gas. From the time dependence of r^2, we extract the asymptotic radial velocity v_r by fitting $\sqrt{r^2} = \sqrt{r_0^2 + v_r^2 t^2}$, where r_0 is the initial size of the cloud [53]. Figure 4 shows v_r as a function of U/J. We find $v_r = 1.40(6) d/\tau$ for $U = 0$ and $U = 20J$, whereas for intermediate interactions $U \sim 3J$, the radial velocity decreases weakly. Note that for $U \gg W$, the mass transport in the 1D FHM in the absence of doublons becomes identical to a noninteracting gas of spinless fermions and thus it behaves exactly like hardcore bosons in 1D with $v_r = \sqrt{2} d/\tau$ [19]. The values in the limiting cases agree with these theoretical predictions for free fermions expanding from our initial state. Remarkably, compared to the Bose-Hubbard model [19], the reduction of v_r at intermediate interaction strengths is much weaker (Fig. 4).

Starting from the limit of very strong interactions, the interaction dependence of v_r can be understood in a

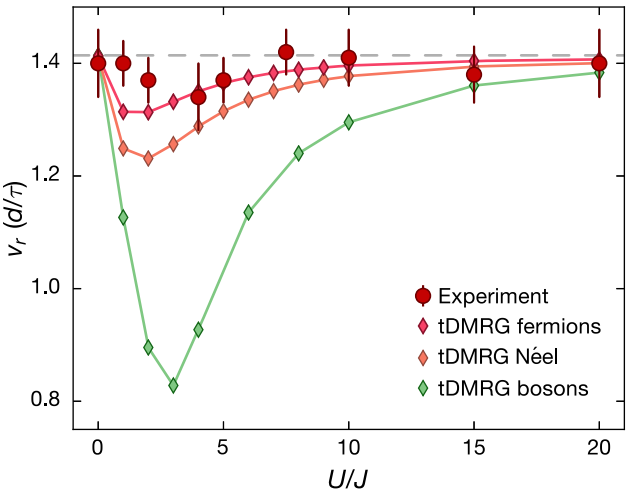

FIG. 4. Radial expansion velocities v_r. Experiment (circles) and tDMRG simulations for fermions (red dark-shaded diamonds) and bosons (green light-shaded diamonds, from Ref. [19]) as a function of U/J. Solid lines are guides to the eye. The grey dashed line indicates $v_r = \sqrt{2} d/\tau$ in the limiting cases $U/J = 0$ and $U/J \to \infty$. All initial states in the numerical simulations have a uniform average density of $n = 1$ in a box with initial size $L_{\text{init}} = 10$.

two-component picture of independent singlon and doublon gases [65,66]: The dynamically generated doublons undergo a quantum distillation mechanism and are then inert on the time scales of the experiment. Thus, the more doublons are generated, the less kinetic energy is available for the rapidly expanding singlons. Focusing on the quantitative difference between the $v_r(U)$ curves for bosons and fermions, which is the main result of the data presented in Fig. 4, two aspects are important. First, in the case of fermions, doublons can only be generated between sites with fermions of *different* spin orientation [33]. The initial state that has the most of such $\uparrow$-$\downarrow$ neighbors is the Néel state, and this initial state leads to the most pronounced minimum of v_r (Fig. 4, [33]). In order to compare to the experiment, we average over many 1D systems with random spin orientations for a balanced spin mixture (dark red diamonds in Fig. 4). This averaging leads to a weaker minimum in v_r than for the Néel state and is in agreement with our experimental data. The second reason for the stronger minimum in v_r for bosons is the fact that the interaction energy can become much larger, since larger local occupancies are possible [19]. In order to test whether the observed v_r can primarily be understood as a function of the interaction energy in the system after the formation of doublons, we show data for different U/J and different spin configurations versus interaction energy in the Supplemental Material (Fig. S8 in Ref. [53]). The data for bosons lie well outside the accessible range of interaction energies for fermions because of higher site occupations, but fall onto an extrapolation of the fermionic data. Hence, the integrability of the 1D FHM does not seem to be the dominant reason for the differences to the bosonic case. An interesting

extension would be the calculation of expansion velocities by exploiting the integrability along the lines of Refs. [35,67], which we leave for future work.

Summary and outlook.—We investigated the sudden expansion of an interacting cloud of fermions. Starting from an initial product state with an appreciable doublon fraction, we observed a dynamical phase separation between singlons and doublons, theoretically known as fermionic quantum distillation in the weak regime. Additionally, we analyzed radial velocities for different interaction strengths using initial states consisting purely of singlons. We found a decrease of the radial velocities at weak interactions and attributed this effect to dynamically generated doublons. The weak decrease of radial velocities of expanding fermions compared to bosons is due to the Pauli principle leading to a crucial dependence of the radial velocities on the initial spin configuration. Future experiments could use the singlon and doublon resolved scheme to detect signatures of FFLO states [67–69] in sudden-expansion experiments. Moreover, it would be intriguing to observe the strong version of quantum distillation, resulting in the dynamical formation of low-entropy regions. This could be achieved by optimizing the initial-state properties and improved imaging techniques, such as microwave dressing to isolate central 1D systems, where the conditions for strong quantum distillation are best, or using quantum-gas microscopes [70,71].

We acknowledge financial support by the European Commission (UQUAM Grant No. 319278, AQuS) and the Nanosystems Initiative Munich (NIM) Grant No. EXC4. J. S. and F. H.-M. were supported by the DFG (Deutsche Forschungsgemeinschaft) Research Unit FOR 1807 under Grant No. HE 5242/3-2 and by startup funds via SFB 1073 at the University of Göttingen. J. H. was supported by the US Department of Energy (DOE), Office of Basic Energy Sciences (BES), Materials Sciences and Engineering Division.

*monika.aidelsburger@physik.uni-muenchen.de

[1] G. Baym and C. Pethick, *Landau Fermi-Liquid Theory* (Wiley, New York, 1991).
[2] T. Giamarchi, *Quantum Physics in One Dimension* (Oxford University Press, New York, 2004).
[3] M. A. Cazalilla, R. Citro, T. Giamarchi, E. Orignac, and M. Rigol, One dimensional bosons: From condensed matter systems to ultracold gases, Rev. Mod. Phys. **83**, 1405 (2011).
[4] A. Klümper, Integrability of quantum chains: Theory and applications to the spin-1/2 XXZ chain, Lect. Notes Phys. **645**, 349 (2004).
[5] F. H. L. Essler, H. Frahm, F. Göhmann, A. Klümper, and V. E. Korepin, *The One-Dimensional Hubbard Model* (Cambridge University Press, Cambridge, England, 2005).
[6] M. Rigol, V. Dunjko, V. Yurovsky, and M. Olshanii, Relaxation in a Completely Integrable Many-Body Quantum System: An ab initio Study of the Dynamics of the Highly Excited States of 1D Lattice Hard-Core Bosons, Phys. Rev. Lett. **98**, 050405 (2007).
[7] L. Vidmar and M. Rigol, Generalized Gibbs ensemble in integrable lattice models, J. Stat. Mech. Theor. Exp. (**2016**) 064007.
[8] T. Kinoshita, T. Wenger, and D. S. Weiss, A quantum Newton's cradle, Nature (London) **440**, 900 (2006).
[9] S. Hofferberth, I. Lesanovsky, B. Fisher, T. Schumm, and J. Schmiedmayer, Non-equilibrium coherence dynamics in one-dimensional Bose gases, Nature (London) **449**, 324 (2007).
[10] M. Gring, M. Kuhnert, T. Langen, T. Kitagawa, B. Rauer, M. Schreitl, I. Mazets, D. A. Smith, E. Demler, and J. Schmiedmayer, Relaxation and prethermalization in an isolated quantum system, Science **337**, 1318 (2012).
[11] T. Langen, S. Erne, R. Geiger, B. Rauer, T. Schweigler, M. Kuhnert, W. Rohringer, I. E. Mazets, T. Gasenzer, and J. Schmiedmayer, Experimental observation of a generalized Gibbs ensemble, Science **348**, 207 (2015).
[12] X. Zotos, F. Naef, and P. Prelovšek, Transport and conservation laws, Phys. Rev. B **55**, 11029 (1997).
[13] F. Heidrich-Meisner, A. Honecker, and W. Brenig, Transport in quasi one-dimensional spin-1/2 systems, Eur. Phys. J. Spec. Top. **151**, 135 (2007).
[14] R. Vasseur and J. E. Moore, Nonequilibrium quantum dynamics and transport: from integrability to many-body localization, J. Stat. Mech. Theor. Exp. (**2016**) 064010.
[15] C. Karrasch, T. Prosen, and F. Heidrich-Meisner, Proposal for measuring the finite-temperature drude weight of integrable systems, Phys. Rev. B **95**, 060406 (2017).
[16] H. Ott, E. de Mirandes, F. Ferlaino, G. Roati, G. Modugno, and M. Inguscio, Collisionally Induced Transport in Periodic Potentials, Phys. Rev. Lett. **92**, 160601 (2004).
[17] N. Strohmaier, Y. Takasu, K. Günter, R. Jördens, M. Köhl, H. Moritz, and T. Esslinger, Interaction-Controlled Transport of an Ultracold Fermi Gas, Phys. Rev. Lett. **99**, 220601 (2007).
[18] U. Schneider, L. Hackermüller, J. P. Ronzheimer, S. Will, S. Braun, T. Best, I. Bloch, E. Demler, S. Mandt, D. Rasch, and A. Rosch, Fermionic transport and out-of-equilibrium dynamics in a homogeneous Hubbard model with ultracold atoms, Nat. Phys. **8**, 213 (2012).
[19] J. P. Ronzheimer, M. Schreiber, S. Braun, S. S. Hodgman, S. Langer, I. P. McCulloch, F. Heidrich-Meisner, I. Bloch, and U. Schneider, Expansion Dynamics of Interacting Bosons in Homogeneous Lattices in One and Two Dimensions, Phys. Rev. Lett. **110**, 205301 (2013).
[20] L. Xia, J. Carrasquilla, A. Reinhard, J. M. Wilson, M. Rigol, and D. S. Weiss, Quantum distillation and confinement of vacancies in a doublon sea, Nat. Phys. **11**, 316–320 (2015).
[21] W. Xu, W. Mcgehee, W. Morong, and B. DeMarco, Bad-Metal Relaxation Dynamics in a Fermi Lattice Gas, arXiv:1606.06669.
[22] R. Anderson, F. Wang, P. Xu, V. Venu, S. Trotzky, F. Chevy, and J. H. Thywissen, Optical conductivity of a quantum gas, arXiv:1712.09965.
[23] P. T. Brown, D. Mitra, E. Guardado-Sanchez, R. Nourafkan, A. Reymbaut, S. Bergeron, A.-M. S. Tremblay, J. Kokalj, D. A. Huse, P. Schauss, and W. S. Bakr, Bad metallic

transport in a cold atom Fermi-Hubbard system, arXiv:1802.09456.
[24] M. A. Nichols, L. W. Cheuk, M. Okan, T. R. Hartke, E. Mendez, T. Senthil, E. Khatami, H. Zhang, and M. W. Zwierlein, Spin transport in a Mott insulator of ultracold fermions, arXiv:1802.10018.
[25] J.-P. Brantut, J. Meineke, D. Stadler, S. Krinner, and T. Esslingerj, Conduction of ultracold fermions through a mesoscopic channel, Science **337**, 1069 (2012).
[26] G. Valtolina, A. Burchianti, A. Amico, E. Neri, K. Xhani, J. A. Seman, A. Trombettoni, A. Smerzi, M. Zaccanti, M. Inguscio, and G. Roati, Josephson effect in fermionic superfluids across the bec-bcs crossover, Science **350**, 1505 (2015).
[27] M. Lebrat, P. Grišins, D. Husmann, S. Häusler, L. Corman, T. Giamarchi, J.-P. Brantut, and T. Esslinger, Band and Correlated Insulators of Cold Fermions in a Mesoscopic Lattice, Phys. Rev. X **8**, 011053 (2018).
[28] M. Rigol and A. Muramatsu, Fermionization in an Expanding 1D gas of Hard-Core Bosons, Phys. Rev. Lett. **94**, 240403 (2005).
[29] A. Minguzzi and D. M. Gangardt, Exact Coherent States of a Harmonically Confined Tonks-Girardeau Gas, Phys. Rev. Lett. **94**, 240404 (2005).
[30] A. del Campo and J. G. Muga, Dynamics of a Tonks-Girardeau gas released from a hard-wall trap, Euro. Phys. Lett. **74**, 965 (2006).
[31] D. Jukić, B. Klajn, and H. Buljan, Momentum distribution of a freely expanding Lieb-Liniger gas, Phys. Rev. A **79**, 033612 (2009).
[32] S. Langer, M. J. A. Schuetz, I. P. McCulloch, U. Schollwöck, and F. Heidrich-Meisner, Expansion velocity of a one-dimensional, two-component Fermi gas during the sudden expansion in the ballistic regime, Phys. Rev. A **85**, 043618 (2012).
[33] L. Vidmar, S. Langer, I. P. McCulloch, U. Schneider, U. Schollwöck, and F. Heidrich-Meisner, Sudden expansion of Mott insulators in one dimension, Phys. Rev. B **88**, 235117 (2013).
[34] A. S. Campbell, D. M. Gangardt, and K. V. Kheruntsyan, Sudden Expansion of a One-Dimensional Bose Gas from Power-Law Traps, Phys. Rev. Lett. **114**, 125302 (2015).
[35] Z. Mei, L. Vidmar, F. Heidrich-Meisner, and C. J. Bolech, Unveiling hidden structure of many-body wave functions of integrable systems via sudden-expansion experiments, Phys. Rev. A **93**, 021607 (2016).
[36] N. Schlünzen, S. Hermanns, M. Bonitz, and C. Verdozzi, Dynamics of strongly correlated fermions: Ab initio results for two and three dimensions, Phys. Rev. B **93**, 035107 (2016).
[37] M. Rigol and A. Muramatsu, Emergence of Quasicondensates of Hard-Core Bosons at Finite Momentum, Phys. Rev. Lett. **93**, 230404 (2004).
[38] I. Hen and M. Rigol, Strongly Interacting Atom Lasers in Three-Dimensional Optical Lattices, Phys. Rev. Lett. **105**, 180401 (2010).
[39] M. Jreissaty, J. Carrasquilla, F. A. Wolf, and M. Rigol, Expansion of Bose-Hubbard Mott insulators in optical lattices, Phys. Rev. A **84**, 043610 (2011).
[40] L. Vidmar, J. P. Ronzheimer, M. Schreiber, S. Braun, S. S. Hodgman, S. Langer, F. Heidrich-Meisner, I. Bloch, and U. Schneider, Dynamical Quasicondensation of Hard-Core Bosons at Finite Momenta, Phys. Rev. Lett. **115**, 175301 (2015).
[41] L. Vidmar, D. Iyer, and M. Rigol, Emergent Eigenstate Solution to Quantum Dynamics Far from Equilibrium, Phys. Rev. X **7**, 021012 (2017).
[42] F. Heidrich-Meisner, S. R. Manmana, M. Rigol, A. Muramatsu, A. E. Feiguin, and E. Dagotto, Quantum distillation: Dynamical generation of low-entropy states of strongly correlated fermions in an optical lattice, Phys. Rev. A **80**, 041603 (2009).
[43] D. Muth, D. Petrosyan, and M. Fleischhauer, Dynamics and evaporation of defects in Mott-insulating clusters of boson pairs, Phys. Rev. A **85**, 013615 (2012).
[44] J. Herbrych, A. E. Feiguin, E. Dagotto, and F. Heidrich-Meisner, Efficiency of fermionic quantum distillation, Phys. Rev. A **96**, 033617 (2017).
[45] K. Winkler, G. Thalhammer, F. Lang, R. Grimm, J. Hecker Denschlag, A. J. Daley, A. Kantian, H. P. Bahler, and P. Zoller, Repulsively bound atom pairs in an optical lattice, Nature (London) **441**, 853 (2006).
[46] R. Rausch and M. Potthoff, Filling-dependent doublon dynamics in the one-dimensional Hubbard model, Phys. Rev. B **95**, 045152 (2017).
[47] J.-S. Bernier, C. Kollath, A. Georges, L. De Leo, F. Gerbier, C. Salomon, and M. Köhl, Cooling fermionic atoms in optical lattices by shaping the confinement, Phys. Rev. A **79**, 061601 (2009).
[48] T.-L. Ho and Q. Zhou, Universal cooling scheme for quantum simulation, arXiv:0911.5506.
[49] A. Mazurenko, C. S. Chiu, G. Ji, M. F. Parsons, M. Kanasz-Nagy, R. Schmidt, F. Grusdt, E. Demler, D. Greif, and M. Greiner, A cold-atom Fermi-Hubbard antiferromagnet, Nature (London) **545**, 462 (2017).
[50] C. S. Chiu, G. Ji, A. Mazurenko, D. Greif, and M. Greiner, Quantum State Engineering of a Hubbard System with Ultracold Fermions, Phys. Rev. Lett. **120**, 243201 (2018).
[51] D. McKay and B. DeMarco, Cooling in strongly correlated optical lattices: prospects and challenges, Rep. Prog. Phys. **74**, 054401 (2011).
[52] F. Heidrich-Meisner, M. Rigol, A. Muramatsu, A. E. Feiguin, and E. Dagotto, Ground-state reference systems for expanding correlated fermions in one dimension, Phys. Rev. A **78**, 013620 (2008).
[53] See the Supplemental Material at http://link.aps.org/supplemental/10.1103/PhysRevLett.121.130402, which includes Refs. [54–62], not cited in the main text, for details on the initial state preparation, the creation of a flat potential, the control of the doublon fraction, the singlon-doublon resolved read-out, the estimation of tubes with few doublons, the fits to the time traces of R_d, as well as the extraction of the radial velocities. Additionally, details of the tDMRG simulations are explained.
[54] U. Schneider, L. Hackermüller, S. Will, Th. Best, I. Bloch, T. A. Costi, R. W. Helmes, D. Rasch, and A. Rosch, Metallic and insulating phases of repulsively interacting fermions in a 3d optical lattice, Science **322**, 1520 (2008).

[55] S. R. White and A. E. Feiguin, Real-Time Evolution using the Density Matrix Renormalization Group, Phys. Rev. Lett. **93**, 076401 (2004).
[56] A. J. Daley, C. Kollath, U. Schollwöck, and G. Vidal, Time-dependent density-matrix renormalization-group using adaptive effective Hilbert spaces, J. Stat. Mech. Theor. Exp. **2004**, P04005.
[57] G. Vidal, Efficient Simulation of One-Dimensional Quantum Many-Body Systems, Phys. Rev. Lett. **93**, 040502 (2004).
[58] U. Schollwöck, The density-matrix renormalization group in the age of matrix product states, Ann. Phys. (Amsterdam) **326**, 96 (2011).
[59] T. Enss and J. Sirker, Light cone renormalization and quantum quenches in one-dimensional Hubbard models, New J. Phys. **14**, 023008 (2012).
[60] A. Bauer, F. Dorfner, and F. Heidrich-Meisner, Temporal decay of Néel order in the one-dimensional Fermi-Hubbard model, Phys. Rev. A **91**, 053628 (2015).
[61] C. Degli Esposti Boschi, E. Ercolessi, L. Ferrari, P. Naldesi, F. Ortolani, and L. Taddia, Bound states and expansion dynamics of interacting bosons on a one-dimensional lattice, Phys. Rev. A **90**, 043606 (2014).
[62] F. Dorfner, Doctoral thesis, Ludwig-Maximilians University Munich, 2016.
[63] A. Rosch, D. Rasch, B. Binz, and M. Vojta, Metastable Superfluidity of Repulsive Fermionic Atoms in Optical Lattices, Phys. Rev. Lett. **101**, 265301 (2008).
[64] M. T. DePue, C. McCormick, S. L. Winoto, S. Oliver, and D. S. Weiss, Unity Occupation of Sites in a 3D Optical Lattice, Phys. Rev. Lett. **82**, 2262 (1999).
[65] J. Kajala, F. Massel, and P. Törmä, Expansion Dynamics in the One-Dimensional Fermi-Hubbard Model, Phys. Rev. Lett. **106**, 206401 (2011).
[66] S. Sorg, L. Vidmar, L. Pollet, and F. Heidrich-Meisner, Relaxation and thermalization in the one-dimensional Bose-Hubbard model: A case study for the interaction quantum quench from the atomic limit, Phys. Rev. A **90**, 033606 (2014).
[67] C. J. Bolech, F. Heidrich-Meisner, S. Langer, I. P. McCulloch, G. Orso, and M. Rigol, Long-Time Behavior of the Momentum Distribution during the Sudden Expansion of a Spin-Imbalanced Fermi Gas in One Dimension, Phys. Rev. Lett. **109**, 110602 (2012).
[68] J. Kajala, F. Massel, and P. Törmä, Expansion dynamics of the Fulde-Ferrell-Larkin-Ovchinnikov state, Phys. Rev. A **84**, 041601 (2011).
[69] H. Lu, L. O. Baksmaty, C. J. Bolech, and H. Pu, Expansion of 1D Polarized Superfluids: The Fulde-Ferrell-Larkin-Ovchinnikov State Reveals Itself, Phys. Rev. Lett. **108**, 225302 (2012).
[70] E. Haller, J. Hudson, A. Kelly, D. A. Cotta, B. Peaudecerf, G. D. Bruce, and S. Kuhr, Single-atom imaging of fermions in a quantum-gas microscope, Nat. Phys. **11**, 738 (2015).
[71] L. W. Cheuk, M. A. Nichols, M. Okan, T. Gersdorf, V. V. Ramasesh, W. S. Bakr, T. Lompe, and M. W. Zwierlein, Quantum-Gas Microscope for Fermionic Atoms, Phys. Rev. Lett. **114**, 193001 (2015).